Forbidden Directions for TM Waves in Anisotropic Conducting Media

José M. Carcione and Fabio Cavallini

***Abstract*— We investigate the wave propagation properties of nonuniform plane waves in an (unbounded homogeneous) anisotropic conducting material. Such waves (for which amplitudes vary across surfaces of constant phase) characterize the refracted field in an imperfect dielectric, like the earth when a uniform electromagnetic plane wave is incident from the air. The results, presented in terms of polar diagrams of the attenuation, slowness, energy velocity, and quality factor predict the existence of "stopbands" beyond a given degree of nonuniformity (i.e., combinations of propagation and attenuation directions where there is no wave propagation). This is a peculiar effect due to the joint presence of anisotropy and conductivity that may have application in the design of synthetic materials acting as absorbers of electromagnetic radiation.**

***Index Terms*—Electromagnetic theory.**

I. Introduction

NONUNIFORM plane waves have the property that planes of constant amplitude do not coincide with planes of constant phase. This implies that the wavevector and the attenuation vector do not have a common direction. These waves are generated at the heterogeneities of the medium. For instance, in the problem of reflection and refraction of plane waves at a boundary between two electrically different half-spaces, the familiar uniform waves (equiphase planes and equiamplitude planes coincide) are not generally enough to satisfy the boundary conditions (e.g., [1]). The problem should include the nonuniform plane waves which characterize the refracted field in an imperfect dielectric like the earth or the sea when a uniform plane wave is incident on its plane boundary from a perfect dielectric like air. Therefore, in layered media these waves are not the exception but the rule.

To our knowledge, little attention has been paid to the propagation of nonuniform waves in anisotropic media. For instance, Born and Wolf [2, p. 708] describe wave propagation in absorbing crystals, but they assume uniform plane waves. Moreover, recent results [3]–[8] dealing with propagation in anisotropic lossy materials do not exhaust the related problems. In viscoelastodynamics, several researchers investigated the problem in the isotropic case, notably Buchen [9] and Borcherdt [10].

Manuscript received October 12, 1994; revised March 19, 1996. This work was supported in part by the European Commission in the framework of the JOULE programme, subprogramme Advanced Fuel Technologies.

The authors are with Osservatorio Geofisico Sperimentale di Trieste, Opicina, 34016 Trieste, Italy.

Publisher Item Identifier S 0018-926X(97)00450-X.

In this work, we consider the propagation of TM (transverse-magnetic) waves in an anisotropic conducting medium. Three variables describe the problem, two electric field components and the magnetic field perpendicular to the propagation plane. From the mathematical point of view, this problem is analogous to that of pure viscoelastic shear waves propagating in the plane of mirror symmetry of a monoclinic medium [11], and generalizes the approach in [12] where homogeneous plane waves were considered.

II. Dispersion Relation for Nonuniform TM Waves

Assume that an electromagnetic wave propagates in the (x, z)-plane, and that the material properties are constant with respect to the y coordinate. Then, the field components E_x, E_z, and H_y are decoupled from E_y, H_x, and H_z. The first three obey the TM (transverse-magnetic) Maxwell differential equations which, in the absence of magnetic moments and electric current sources, can be written in compact form as

$$\nabla_2^\top \bullet \mathbf{E} = \mu \frac{\partial H_y}{\partial t} \tag{1}$$

$$\nabla_2 H_y = \boldsymbol{\sigma} \bullet \mathbf{E} + \boldsymbol{\epsilon} \bullet \frac{\partial \mathbf{E}}{\partial t} \tag{2}$$

where $\mathbf{E} = [E_x, E_z]^\top$, $\nabla_2 = [-\partial/\partial z, \partial/\partial x]^\top$, while

$$\boldsymbol{\epsilon} = \begin{bmatrix} \epsilon_{11} & 0 \\ 0 & \epsilon_{33} \end{bmatrix}$$
$$\boldsymbol{\sigma} = \begin{bmatrix} \sigma_{11} & 0 \\ 0 & \sigma_{33} \end{bmatrix} \tag{3}$$

are the permittivity and conductivity matrices both expressed in the principal coordinate system of the medium. The symbol $\bullet$ denotes ordinary matrix multiplication.

The magnetic field associated to a nonuniform TM plane wave has the form

$$\mathbf{H} = H_y \hat{\mathbf{e}}_y$$
$$H_y \equiv H_0 e^{i(\omega t - \mathbf{k} \bullet \mathbf{x})}$$
$$\hat{\mathbf{e}}_y \equiv [0, 1, 0]^\top \tag{4}$$

where $\mathbf{x} = (x, z)$, H_0 is a complex constant, and $\mathbf{k} = \boldsymbol{\kappa} - i\boldsymbol{\alpha}$ is the complex wavevector with $\boldsymbol{\kappa}$ and $\boldsymbol{\alpha}$ the real propagation and attenuation vectors, respectively. Note that for a nonuniform plane wave, the propagation and attenuation directions do

not coincide. Alternatively, the wavevector can be written as $\mathbf{k} = [k_x, k_z]$, where k_x and k_z are complex components.

Since for the plane wave (4), the operator ∇_2 is

$$\nabla_2 = -i\mathbf{K}_2 \qquad \mathbf{K}_2 \equiv \begin{bmatrix} -k_z \\ k_x \end{bmatrix} \tag{5}$$

substitution of (5) into (1) and (2) yields, after some algebra, the dispersion relation

$$\mathbf{K}_2^{\top} \bullet \boldsymbol{\beta} \bullet \mathbf{K}_2 - \mu\omega^2 = 0 \tag{6}$$

where

$$\boldsymbol{\beta} \equiv \begin{bmatrix} \beta_{11} & 0 \\ 0 & \beta_{33} \end{bmatrix} \equiv \left(\boldsymbol{\epsilon} - \frac{i}{\omega}\boldsymbol{\sigma} \right)^{-1} \tag{7}$$

is the dielectric impermeability matrix. In components, (6) becomes

$$\beta_{33}\, k_x^2 + \beta_{11}\, k_z^2 - \mu\omega^2 = 0 \tag{8}$$

where

$$\beta_{11} = \left(\epsilon_{11} - \frac{i}{\omega}\sigma_{11} \right)^{-1}$$

and

$$\beta_{33} = \left(\epsilon_{33} - \frac{i}{\omega}\sigma_{33} \right)^{-1}. \tag{9}$$

From (2) and using (7), the electric field can be written as

$$\mathbf{E} = -\frac{H_y}{\omega}(\boldsymbol{\beta} \bullet \mathbf{K_2}). \tag{10}$$

III. Kinematics of the Wave Propagation

The components of the complex wavevector $\boldsymbol{\kappa}$ can be written as

$$k_x = \kappa l_x - i\alpha m_x$$

and

$$k_z = \kappa l_z - i\alpha m_z \tag{11}$$

where $[m_x, m_z]^{\top} \equiv \hat{\boldsymbol{\alpha}}$ defines the attenuation direction, and $\hat{\boldsymbol{\kappa}} = [l_x, l_z]^{\top}$ holds together with $\boldsymbol{\kappa} = \kappa\hat{\boldsymbol{\kappa}}$. The propagation and attenuation unit vectors can be expressed in terms of propagation and nonuniformity angles θ and γ as

$$l_x = \sin\theta \qquad l_z = \cos\theta \tag{12}$$

$$m_x = \sin(\theta + \gamma) \qquad m_z = \cos(\theta + \gamma) \tag{13}$$

where $\gamma = \arccos(\hat{\boldsymbol{\kappa}} \bullet \hat{\boldsymbol{\alpha}})$. We consider here that $-90° \leq \gamma \leq 90°$, i.e., the amplitude decreases in equiphase planes, although the values $\gamma = \pm 90°$ are forbidden in the dissipative isotropic case [13, p. 141]. The problem is now to express the real wavenumber and attenuation factors κ and α in terms of the angular frequency ω and the directions $\hat{\boldsymbol{\kappa}}$ and $\hat{\boldsymbol{\alpha}}$. Substituting the wavevector components (11) into the dispersion relation (8) and reordering terms gives

$$a\kappa^2 - b\alpha^2 - 2ic\kappa\alpha = \omega^2 \tag{14}$$

where

$$\mu a = \beta_{33} l_x^2 + \beta_{11} l_z^2 \tag{15}$$

$$\mu b = \beta_{33} m_x^2 + \beta_{11} m_z^2 \tag{16}$$

$$\mu c = \beta_{33} l_x m_x + \beta_{11} l_z m_z. \tag{17}$$

The imaginary part of (14) yields the following relationship between κ and α:

$$\alpha = q\kappa \qquad q \equiv \frac{a_I}{c_R + (c_R^2 + a_I b_I)^{1/2}} \tag{18}$$

where the subscripts R and I denote real and imaginary parts, respectively. Substituting relation (18) into the real part of (14) gives the expression for the real wavenumber

$$\kappa = \frac{\omega}{(a_R - q^2 b_R + 2q c_I)^{1/2}}. \tag{19}$$

Note that $a_R - q^2 b_R + 2q c_I \equiv V_p^2$ is the square of the phase velocity, and must be a positive quantity. Therefore, the real wavenumber and attenuation vectors are

$$\boldsymbol{\kappa} = \kappa\hat{\boldsymbol{\kappa}} \qquad \boldsymbol{\alpha} = q\kappa\hat{\boldsymbol{\alpha}}. \tag{20}$$

The slowness vector and the phase velocity vector are

$$\mathbf{s} = \frac{\kappa}{\omega}\hat{\boldsymbol{\kappa}} \qquad \mathbf{V}_p = \frac{\omega}{\kappa}\hat{\boldsymbol{\kappa}}. \tag{21}$$

Mathematically, it is possible for V_p^2 to be negative for given values of the variables θ, γ, and ω. As we shall see in the examples, these solutions give rise to forbidden propagation directions or "stopbands."

IV. Energy Analysis

The group velocity is much simpler to compute than the energy velocity which involves the calculation of the Umov–Poynting vector and energy densities. Moreover, as in the acoustic case the group velocity equals the energy velocity when there is no attenuation, i.e., for a perfectly dielectric medium.

However, the description of the wavefront requires the explicit calculation of the energy velocity since the concept of group velocity looses its physical meaning when the attenuation is relatively high [12], [14].

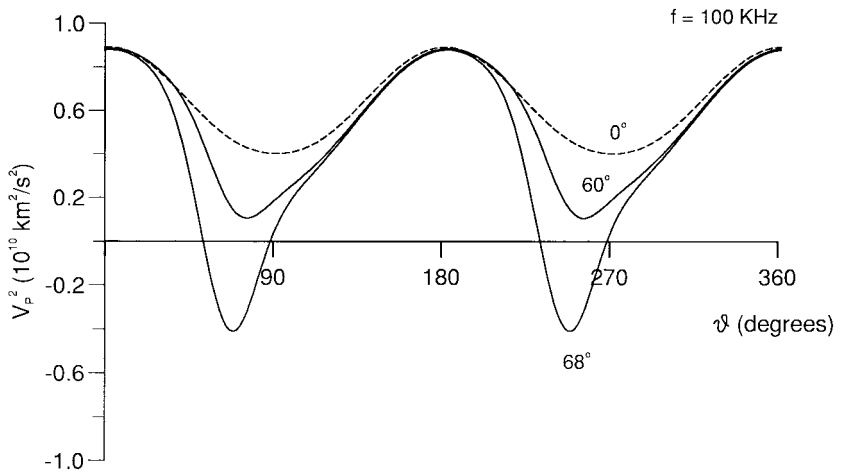

Fig. 1. Square of the phase velocity as a function of the propagation angle θ for three values of the nonuniformity angle γ. The broken lines correspond to uniform plane waves. As can be seen, when $\gamma = 68^\circ$, the phase velocity is pure imaginary for two ranges of propagation angles (stopbands).

A. Complex Umov–Poynting Theorem

The energy balance equation for three-dimensional (3-D) nonuniform plane waves in the absence of magnetic moments and electric currents is (e.g., [15])

$$\nabla \bullet \mathbf{P} - 2i\omega[(w_e)_{AV} - (w_m)_{AV}] + (p_d)_{AV} = 0 \qquad (22)$$

where $\mathbf{P}$ is the complex Umov–Poynting vector

$$\mathbf{P} \equiv \tfrac{1}{2}(\mathbf{E} \times \mathbf{H}^*) = \tfrac{1}{2}H_y^* \begin{bmatrix} -E_z \\ E_x \end{bmatrix} \qquad (23)$$

with the asterisk denoting complex conjugation. The real part of the Umov–Poynting vector gives the average power flow density over a cycle. By substituting (10) into (23), the mean power-flow density becomes

$$\Re(\mathbf{P}) = \frac{1}{2}\frac{|H_0|^2}{\omega} e^{-2\boldsymbol{\alpha}\bullet\mathbf{x}} \Re(\beta_{33} k_x \mathbf{e}_1 + \beta_{11} k_z \mathbf{e}_3) \qquad (24)$$

where (4) has been used. The quantities

$$\begin{aligned} (w_e)_{AV} &= \tfrac{1}{4}\Re[(\mathbf{E}^*)^\top \bullet \mathbf{D}] \\ (w_m)_{AV} &= \tfrac{1}{4}\Re[(\mathbf{H}^*)^\top \bullet \mathbf{B}] \end{aligned} \qquad (25)$$

are the time-average electric and magnetic energy densities, where $\mathbf{D} = \boldsymbol{\epsilon} \bullet \mathbf{E}$ is the electric flux density and $\mathbf{B} = \mu\mathbf{H}$ is the magnetic flux density [16]. Moreover

$$(p_d)_{AV} = \tfrac{1}{2}\Re[(\mathbf{E}^*)^\top \bullet \mathbf{J}] \qquad (26)$$

is the time-average dissipated power density, where $\mathbf{J} = \boldsymbol{\sigma} \bullet \mathbf{E}$.

For nonuniform plane waves of the form (4), the Poynting theorem (22) becomes

$$2\boldsymbol{\alpha}^\top \bullet \mathbf{P} + 2i\omega[(w_e)_{AV} - (w_m)_{AV}] - (p_d)_{AV} = 0. \qquad (27)$$

In (27), we use the two-dimensional notation for vectors and for the matrix product. A similar energy balance equation was obtained by Carcione and Cavallini [17] for viscoelastic inhomogeneous plane waves. Many of the fundamental relations obtained in [17] also hold for electromagnetic nonuniform wave fields if one invokes the acoustic-electromagnetic analogy [18].

In the following paragraphs, the Umov–Poynting vector and energy densities for TM waves are calculated and then used to compute the energy velocity and the quality factor.

B. Energy Velocity and Wavefront

The energy velocity $\mathbf{V}_e$ is the ratio between the average power flow $\Re(\mathbf{P})$ and the mean energy density $(w)_{AV} = (w_e + w_m)_{AV}$ [13]. Hence

$$\mathbf{V}_e = \frac{\Re(\mathbf{P})}{(w_e + w_m)_{AV}}. \qquad (28)$$

On the other hand, from (10), (25), and using $\mathbf{D} = \boldsymbol{\epsilon} \bullet \mathbf{E}$, the electric energy density is

$$(w_e)_{AV} = \frac{1}{4}\frac{|H_0|^2}{\omega^2} e^{-2\boldsymbol{\alpha}\bullet\mathbf{x}} \Re[(\mathbf{K}_2^*)^\top \bullet \boldsymbol{\beta}^* \bullet \boldsymbol{\epsilon} \bullet \boldsymbol{\beta} \bullet \mathbf{K}_2] \qquad (29)$$

where the fact that $\boldsymbol{\beta}$ is a symmetric matrix has been used. Taking into account that $\boldsymbol{\epsilon} = \Re(\boldsymbol{\beta}^{-1})$ and (7), it is easy to show that $\boldsymbol{\beta}^* \bullet \boldsymbol{\epsilon} \bullet \boldsymbol{\beta} = \Re(\boldsymbol{\beta})$. Then

$$(w_e)_{AV} = \frac{1}{4}\frac{|H_0|^2}{\omega^2} e^{-2\boldsymbol{\alpha}\bullet\mathbf{x}} \Re[\beta_{11}|k_z|^2 + \beta_{33}|k_x|^2]. \qquad (30)$$

Replacing the wavevector components (11) into (30), and using (15), (16), (18), and (21), the electric energy density becomes

$$(w_e)_{AV} = \frac{1}{4}\mu\frac{|H_0|^2}{V_p^2} e^{-2\boldsymbol{\alpha}\bullet\mathbf{x}} \Re[a + q^2 b]. \qquad (31)$$

From (25) and using $\mathbf{B} = \mu\mathbf{H}$, the magnetic energy density is

$$(w_m)_{AV} = \frac{1}{4}\mu|H_0|^2 e^{-2\boldsymbol{\alpha}\bullet\mathbf{x}}. \qquad (32)$$

Substitution of the Umov–Poynting vector (24), and the energy

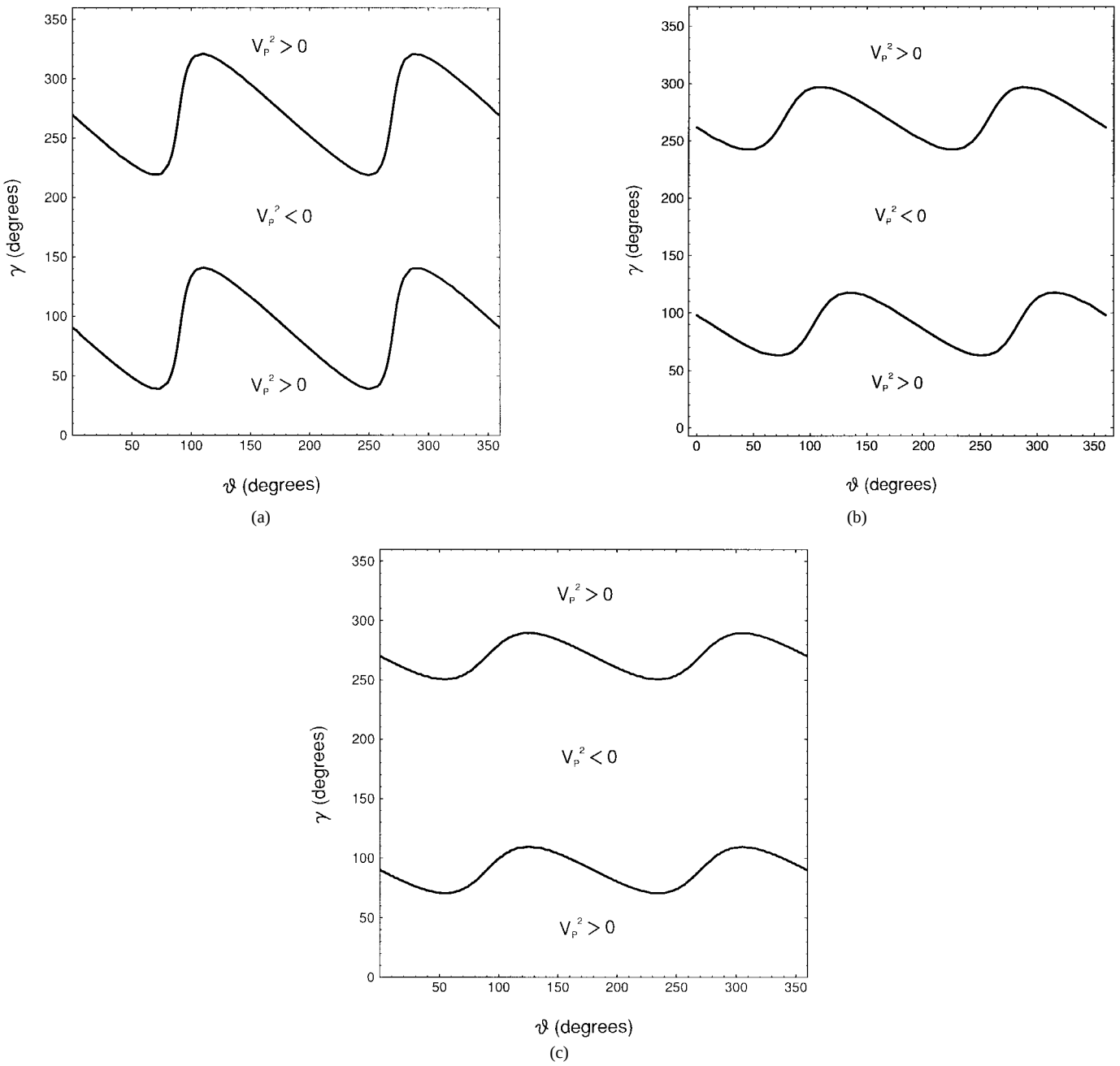

Fig. 2. Zero level contour line of the phase velocity for three different frequencies: (a) 1 kHz, (b) 100 kHz, and (c) 10 MHz.

densities (31) and (32) into (28), gives the energy velocity for nonuniform TM waves

$$\mathbf{V}_e = \frac{2\Re(\beta_{33}k_x\mathbf{e}_1 + \beta_{11}k_z\mathbf{e}_3)}{\mu\omega[1 + V_p^{-2}\Re(a + q^2 b)]}. \tag{33}$$

The location of the energy defines the wavefront. Therefore, the latter is the locus of the tip of the energy velocity vector at unit propagation time.

C. Quality Factor

The quality factor classifies, somehow, matter from the electric current standpoint. As stated by Harrington [19, p. 28], the quality factor is defined as the magnitude of reactive current density to the magnitude of dissipative current density. The concept of quality factor can be considered as a generalization of the concept of Q in circuit theory. Good dielectrics have high Q values, and conductors have very low Q values. In viscoelastodynamics, a definition of quality factor is given by twice the ratio between the average potential energy density and the dissipated energy density. Accordingly, here we define

$$Q = 2\omega\frac{(w_e)_{AV}}{(p_d)_{AV}}. \tag{34}$$

Using (26) and $\mathbf{J} = \boldsymbol{\sigma} \bullet \mathbf{E}$, following the same steps used to obtain the electric energy density, and noting that $\boldsymbol{\sigma} = -\omega\Im(\boldsymbol{\beta}^{-1})$ and $\boldsymbol{\beta}^* \bullet \boldsymbol{\sigma} \bullet \boldsymbol{\beta} = \omega\Im(\boldsymbol{\beta})$, the dissipated power

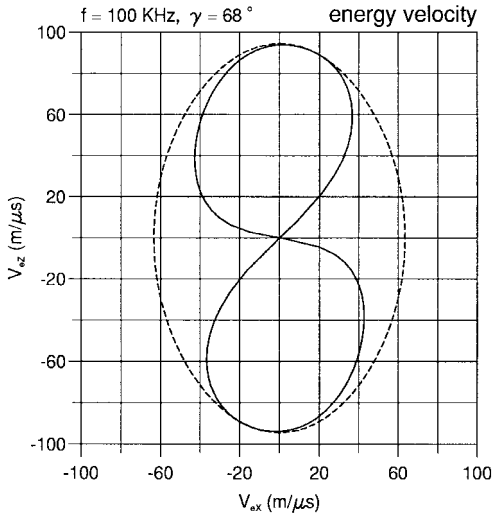

Fig. 3. Polar representations of the energy velocity for a nonuniform plane wave. The broken lines correspond to uniform plane waves ($\gamma = 0°$). Here also, as in Fig. 1, the stopbands can be appreciated. For higher frequencies the bands tend to disappear. In this case, the bands can be activated by increasing the inhomogeneity angle γ.

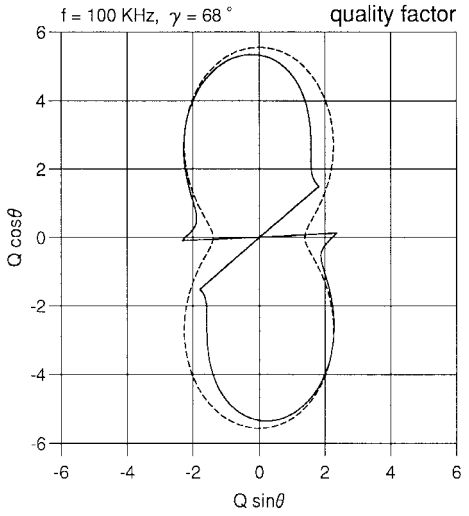

Fig. 4. Polar representations of the quality factor for a nonuniform plane wave. The broken lines correspond to uniform plane waves ($\gamma = 0°$). The quality factor vanishes inside the bands, implying infinite dissipation.

density is written as

$$(p_d)_{AV} = \frac{1}{2}\,\mu\omega\frac{|H_0|^2}{V_p^2}e^{-2\boldsymbol{\alpha}\bullet\mathbf{x}}\Im[a+q^2b]. \tag{35}$$

From the energy densities (31) and (35), definition (34) yields

$$Q = \frac{\Re(a+q^2b)}{\Im(a+q^2b)}. \tag{36}$$

For uniform waves, (36) simply gives $Q = \Re(V^2)/\Im(V^2)$.

V. Examples

We consider an anisotropic medium with $\epsilon_{11} = 10\,\epsilon_0$, $\epsilon_{33} = 20\,\epsilon_0$, where $\epsilon_0 = 8.85\times10^{-12}$ F·m^{-1}, and $\sigma_{11} = 10^{-5}$ S·m^{-1}, $\sigma_{33} = 8\times10^{-5}$ S·m^{-1}. The magnetic permeability μ has been taken equal to that of vacuum ($\mu_0 = 4\pi\times10^{-7}$ H·m^{-1}).

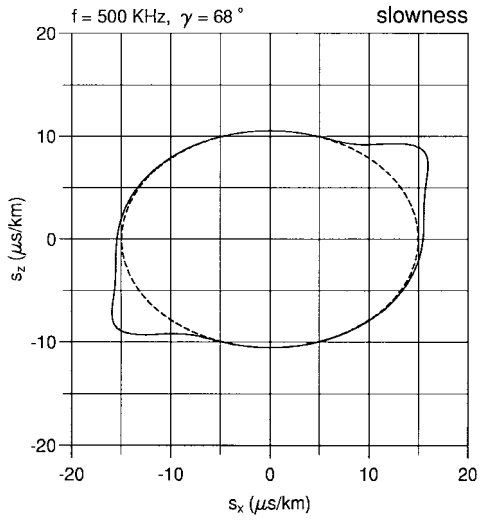

(a)

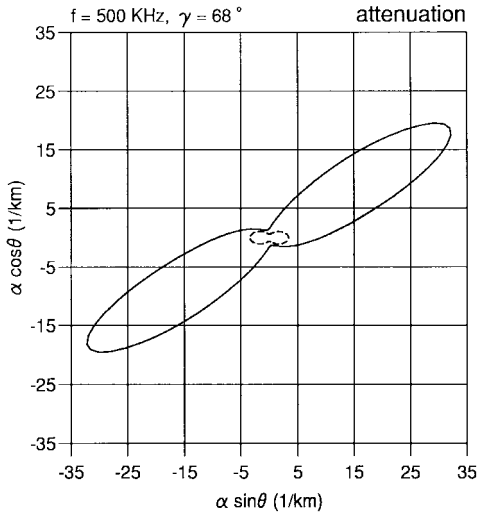

(b)

Fig. 5. Slowness and attenuation. Polar representations of (a) the slowness and (b) the attenuation for a nonuniform plane wave. The broken line corresponds to the uniform plane wave ($\gamma = 0°$).

Fig. 1 represents the square of the phase velocity V_p^2 as a function of the propagation angle θ for a frequency of 100 kHz. The broken line corresponds to the uniform wave ($\gamma = 0$). In the transition from $\gamma = 60°$ to $\gamma = 68°$, two stopbands develop where the wave does not propagate. These bands (intervals in the θ-axis where, for a given frequency and nonuniformity angle, $V_p^2 \leq 0$) are exclusive to conducting anisotropic media—they do not exist in conducting isotropic and in purely dielectric materials. The physical interpretation of this phenomenon requires some considerations. Nonuniform waves are generated at a boundary between two dissimilar media and, therefore, their characteristic parameters are governed by Snell's law. The fact that V_P^2 becomes negative and that, hence, κ becomes purely imaginary (in contradiction with the starting assumption) means that $\boldsymbol{\kappa}$ and $\boldsymbol{\alpha}$ interchange their

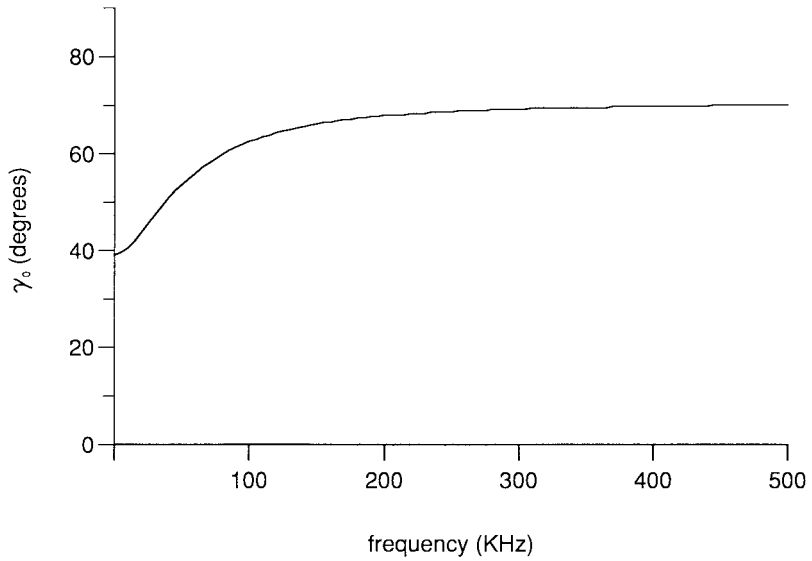

Fig. 6. Nonuniformity threshold versus frequency. The quantity γ_0 is the minimum angle for which the bands are activated (i.e., when, for instance, the phase velocity vanishes).

roles. However, this conversion can never take place, because the generation of such a wave is precluded by Snell's law.

In virtue of the mathematical similarity between the electromagnetic and acoustic problems [11], a similar phenomenon is verified in anisotropic and viscoelastic media [20], [21].

It is then of interest to consider the set of all pairs (θ, γ) where, for a given frequency the propagation is forbidden. This is done in Fig. 2, that shows the contour line $V_p^2(\theta, \gamma) = 0$ for three different frequencies: (a) 1 kHz, (b) 100 kHz, and (c) 10 MHz. For completeness, we have represented the angle γ in the whole mathematical range [0, 360] degrees, but as noted before, the physical ranges are [0, 90] and [270, 360] degrees. As can be observed, the range of γ angles for which stopbands exist is wider for lower frequencies.

Figs. 3 and 4 illustrate energy-related quantities. Fig. 3 shows polar representations of the energy velocity for $\gamma = 68°$ and a frequency of 100 kHz. As before, the broken line corresponds to the uniform wave. Within the stopbands, the energy velocity has been taken as zero. For higher frequencies, the bands may still be present for higher nonuniformity angles. Fig. 4 shows polar representations of the quality factor for $\gamma = 68°$ and a frequency of 100 kHz. As with the energy velocity, the quality factor has been set to zero when the phase velocity is complex.

The slowness and attenuation polar plots for a frequency of 500 kHz are represented in Fig. 5(a) and (b), respectively. Even if there are not stopbands in this case, the attenuation increases substantially with respect to the uniform plane wave case. As expected, the slowness also increases along the same directions.

Given the existence of forbidden propagation directions, it is interesting to consider, for any given frequency f, the threshold nonuniformity angle $\gamma_0(f) \equiv \inf\{\gamma : \exists \theta, V_p^2(\theta, \gamma) < 0\} = \min\{\gamma : \exists \theta, V_p^2(\theta, \gamma) = 0\}$, which can be computed by using the Lagrange multiplier method for finding the minimum of $y(\theta, \gamma) \equiv \gamma$ under the constraint $V_p^2(\theta, \gamma) = 0$. In other words, if the nonuniformity angle γ is greater than $\gamma_0(f)$, then certain propagation angles θ are forbidden. An example of the graph of $\gamma_0(f)$ is shown in Fig. 6. In the diffusion regime, the threshold is lower than in the wave propagation regime, whereas it approaches a constant value in the high-frequency limit.

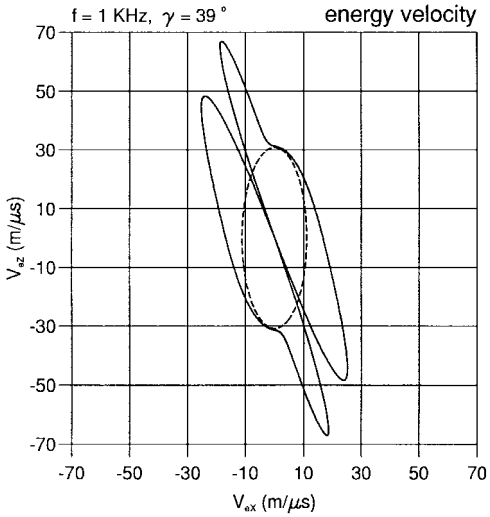

Fig. 7. Polar representation of the energy velocity for a nonuniform plane wave. The broken line corresponds to the uniform plane wave. As expected, in the transition from the wave propagation to the diffusion regime, the energy velocity of the uniform plane wave has substantially decreased (compare with Fig. 3). Moreover, the energy velocity of the nonuniform plane wave shows a strong anisotropic behavior.

Finally, we illustrate the behavior of the energy velocity when the frequency range is approaching the diffusion regime, and the nonuniformity angle is very close to the threshold. Fig. 7 displays a polar representation of the energy velocity for a frequency of 1 kHz and a nonuniformity angle of 39°. The main features are the strong direction dependence of the nonuniform plane wave and the expected contraction of the curve corresponding to the uniform wave. Contrarily to Fig. 3, the velocity of the nonuniform wave is, for most directions, higher than the velocity of the uniform wave.

VI. Conclusions

We considered the propagation of nonuniform plane TM waves in a conducting anisotropic medium. Increasing values of γ (the angle between the propagation and attenuation directions) which is a property of the wave, introduce more dissipation and anisotropy besides the intrinsic properties that the medium shows when probed with uniform waves. In fact, while wavefronts based on the uniformity assumption may appear isotropic, wavefronts composed of nonuniform waves can show a high degree of anisotropy. Furthermore, beyond a given degree of nonuniformity, the combined dissipative-anisotropic properties of the medium give rise to stopbands where there is no propagation at all. It can be shown that the location and width of the bands depend on the material properties, more precisely on the degree of conductivity and anisotropy. It is also remarkable that, contrary to the isotropic case, nonuniform body waves can propagate even for perpendicular propagation and attenuation directions.

A physical interpretation seems to be in order here. The bands correspond to nonphysical solutions, since the phase velocity vanishes or is pure imaginary. A zero phase velocity corresponds to an infinite slowness, but the generation of a wave with such slowness is precluded. The same applies when the slowness takes an imaginary value. However, the effects of the bands should be observable near the threshold, that is when the value of the nonuniformity angle is such that the phase velocity is small and the slowness is high along a given direction. Indeed, this is combined with a high attenuation which produces a substantial dissipation of the wavefield along the band directions; this anomalous highly anisotropic attenuation is really an observable effect. This phenomenon may have application in the design of synthetic materials acting as absorbers of electromagnetic radiation, e.g., optically invisible media. Also, the concept can be used to reduce radar reflections from obstacles.

Numerical modeling of Maxwell's equations [18] is essential to get more physical insight into the dynamics underlying the dispersion relation.

References

[1] R. W. P. King, M. Owens, and T. T. Wu, *Lateral Electromagnetic Waves.* New York: Springer-Verlag, 1992.

[2] M. Born and E. Wolf, *Principles of Optics.* Oxford: Pergamon Press, 1975.

[3] I. V. Lindell, *Methods for Electromagnetic Field Analysis.* Oxford: Clarendon Press, 1992.

[4] J.-J. Angélini, C. Soize, and P. Soudais, "Hybrid numerical method for harmonic 3-D Maxwell equations: Scattering by a mixed conducting and inhomogeneous anisotropic dielectric medium," *IEEE Trans. Antennas Propagat.*, vol. 41, pp. 66–76, Jan. 1993.

[5] J. Schneider and S. Hudson, "The finite-difference time-domain method applied to anisotropic material," *IEEE Trans. Antennas Propagat.*, vol. 41, pp. 994–999, July 1993.

[6] M.-S. Lin, C.-M. Lin, R.-B. Wu, and C. H. Chen, "Transient propagation in anisotropic laminated composites," *IEEE Trans. Electromagn. Compat.*, vol. 35, pp. 357–365, Aug. 1993.

[7] M.-S. Lin, R.-B. Wu, and C. H. Chen, "Time-domain analysis of propagation in inhomogeneous anisotropic lossy slabs," *IEEE Trans. Antennas Propagat.*, vol. 41, pp. 1456–1459, Oct. 1993.

[8] S. He, "The correct ETLC model for anisotropic lossy materials—A comment on 'Transient propagation in anisotropic laminated composites'," *IEEE Trans. Electromagn. Compat.*, vol. 36, pp. 409–410, Nov. 1994.

[9] P. W. Buchen, "Plane waves in linear viscoelastic media," *Geophys. J. Roy. Astr. Soc.*, vol. 23, pp. 531–542, 1971.

[10] R. D. Borcherdt, "Reflection and refraction of type-II S waves in elastic and anelastic solid," *Bull. Seis. Soc. Amer.*, vol. 67, pp. 43–67, 1977.

[11] J. M. Carcione and F. Cavallini, "On the acoustic-electromagnetic analogy," *Wave Motion*, vol. 21, pp. 149–162, 1995.

[12] J. M. Carcione, "Wave fronts in dissipative anisotropic media," *Geophys.*, vol. 59, pp. 644–657, 1994.

[13] H. C. Chen, *Theory of Electromagnetic Fields.* New York: McGraw-Hill, 1983.

[14] K. E. Oughstun and G. C. Sherman, *Electromagnetic Pulse Propagation in Causal Dielectrics.* Berlin: Springer-Verlag, 1994.

[15] H. G. Booker, *Energy in Electromagnetism.* New York: Peregrinus, IEE Electromagn. Waves Ser. 13, 1982.

[16] W. C. Chew, *Waves and Fields in Inhomogeneous Media.* New York: Van Nostrand Reinhold, 1990.

[17] J. M. Carcione and F. Cavallini, "Energy balance and fundamental relations in anisotropic viscoelastic media," *Wave Motion*, vol. 18, pp. 11–20, 1993.

[18] ———, "Modeling transverse electromagnetic waves in conducting anisotropic media by a spectral time-domain technique," *10th Ann. Rev. Progress Appl. Computat. Electromagn.*, vol. II, pp. 586–593, 1994.

[19] R. F. Harrington, *Time-Harmonic Electromagnetic Fields.* New York: McGraw-Hill, 1961.

[20] E. S. Krebes and L. H. T. Le, "Inhomogeneous plane waves and cylindrical waves in anisotropic anelastic media," *J. Geophys. Res.*, vol. 99, pp. 23899–23919, 1994.

[21] J. M. Carcione and F. Cavallini, "Forbidden directions for inhomogeneous pure shear waves in dissipative anisotropic media," *Geophys.*, vol. 60, pp. 522–530, 1995.

José M. Carcione was born in Argentina in 1953. He received the degree "Licenciado in Ciencias Fisicas" from Buenos Aires University, Argentina, in 1978, the degree "Dottore in Fisica" from Milan University, Italy, in 1984, and the Ph.D. in geophysics from Tel-Aviv University, Israel, in 1987.

From 1978 to 1980, he worked at the Comisión Nacional de Energía Atómica, Buenos Aires, Argentina. From 1981 to 1987, he worked as a Research Geophysicist at Yacimientos Petrolíferos Fiscales, Buenos Aires, Argentina. Presently, he is Dirigente di Ricerca at the Osservatorio Geofisico Sperimentale, Trieste, Italy. His current research deals with numerical modeling and the theory of wave propagation in acoustic and electromagnetic media, and their application to geophysical problems and rock physics.

Dr. Carcione was awarded the Alexander von Humboldt scholarship to work at the Geophysical Institute of Hamburg University, in 1989.

Fabio Cavallini was born in 1949. He received the Dottore in Fisica degree (cum laude) in physics from the University of Trieste, Italy, in 1975.

After 1975, he obtained a research scholarship in system theory at the International Center for Mechanical Sciences, Udine, Italy, worked as a Teaching Assistant at the Electronic Engineering Department of the University of Trieste, Italy, and followed graduate courses in functional analysis and its applications at the International School for Advanced Studies in Trieste. Since 1982, he has been working as a Tenure Researcher at the Geophysical Observatory in Trieste, mainly on data processing, numerical modeling, and theory in oceanography, ecology, hydrology, and seismic and electromagnetic waves.